# Active erosion–deposition cycles in the hyperarid Atacama Desert of Northern Chile

Matthew C. Jungers [a,*], Arjun M. Heimsath [a], Ronald Amundson [b], Greg Balco [c], David Shuster [c,d], Guillermo Chong [e]

[a] School of Earth and Space Exploration, Arizona State University, ISTB4, 781 E. Terrace Road Tempe, Room 795, AZ 85287, USA
[b] Department of Environmental Science, Policy and Management, University of California, 137 Mulford Hall, Berkeley, CA 94720, USA
[c] Berkeley Geochronology Center, 2455 Ridge Road, Berkeley, CA 94709, USA
[d] Department of Earth and Planetary Science, University of California, 479 McCone Hall, Berkeley, CA 94720, USA
[e] Departamento de Ciencias Geológicas, Universidad Católica del Norte, Antofagasta, Chile

## ARTICLE INFO

## ABSTRACT

There is significant debate over the rates and types of fluvial activity at the Plio-Pleistocene boundary in the hyperarid Atacama Desert of Chile. To quantify fluvial processes and help resolve this debate, we measure terrestrial cosmogenic nuclide (TCN) ($^{10}$Be and $^{21}$Ne) concentration depth profiles in three settings representing a chronosequence: (1) a late Pliocene alluvial fan representative of major regional deposits, (2) a modern, active channel and (3) an adjacent low terrace inset into the Pliocene alluvium. Late Pliocene deposits that are widely preserved in the region contain TCN profiles consistent with relatively rapid stripping of upland sediment at the Plio-Pleistocene boundary. Deposits inset into these Late Pliocene features record cut and fill cycles that rework sediment throughout the Quaternary. The TCN profile in the modern channel is best explained by sediment aggradation at 2.1 m Myr$^{-1}$ during the last 250,000 yr. Similarly, the adjacent low terrace sediments contain TCN concentration profiles consistent with aggradation of 2.0 m Myr$^{-1}$ over a period of 250,000–750,000 yr prior to the last 250,000 yr of stability. In summary, depth profiles of two TCNs provide constraints on the rates of sediment deposition, sources of sediment and transport history, as well as the subsequent exposure conditions of the sediment following deposition. Our results are consistent with early Quaternary initiation of hyperaridity for the region. During the Quaternary, winter precipitation events experienced at our sites' latitude (24°S) drive active erosion–deposition cycles. The northward migration of the subtropical front during Quaternary glacial cycles may have enhanced precipitation at 24°S, leading to more active fluvial processes during cooler periods.

## 1. Introduction

Alluvial landforms of the Atacama Desert of Chile are widely dominated by pre-Pleistocene deposits, and the hyperarid region is remarkable for the modest to negligible Quaternary modification of the landscape (e.g., Dunai et al., 2005). Landscape reconstructions indicate that prominent Miocene and Pliocene alluvial deposits represent large regional erosion/depositional events, whereas Quaternary processes have locally incised into or lap over these regional fluvial deposits (Amundson et al., 2012). Additionally, bedrock hillslopes are covered with dust and salt, and are in large part isolated from present drainage networks. As a result, Quaternary channels are typically left to rework sediment eroded from adjacent Pliocene and Miocene deposits rather than sediment produced from bedrock or saprolite in an actively eroding upland. Constraints on the magnitudes, frequencies and rates of fluvial processes are sparse.

The proposed change in magnitude and nature of the post-Pliocene, Quaternary sedimentary processes in the Atacama Desert should be recorded in terrestrial cosmogenic nuclide (TCN) surface concentrations, as well as in the TCN depth profiles observed in fluvial deposits. Prior work in the Atacama Desert focused on the exposure ages of surface clasts (Dunai et al., 2005; Nishiizumi et al. 2005; Ewing et al., 2006; Gonzalez et al., 2006; Carrizo et al., 2008; Evenstar et al., 2009; Placzek et al., 2010). We show, however, that depth profiles of TCNs, particularly $^{10}$Be and $^{21}$Ne, provide additional and novel insights into the transport and deposition history of sampled sediment.

To further quantify rates of fluvial processes in the Atacama Desert, we present a dataset of in-situ produced cosmogenic $^{10}$Be and $^{21}$Ne concentration depth profiles in alluvial sediments from

the central Atacama Desert that include the regional late Pliocene deposits and younger, localized Quaternary fluvial features inset into this regional landform. To interpret these data, we (1) compare surface concentrations of cosmogenic nuclides to depth profiles, (2) investigate the complexity of sediment exposure histories, and (3) use cosmogenic nuclides to quantify Quaternary deposition in active channels.

### 1.1. Setting

The Atacama Desert spans approximately 8–10° of latitude within the structurally defined Central Depression of Northern Chile. Three factors are commonly cited as the cause for the region's extreme lack of precipitation: (1) the rain shadow of the Andes to the east, blocking moisture from the Atlantic Ocean; (2) the region's position within the subtropical high-pressure belt; and (3) the upwelling of cold water to the west related to the Pacific Ocean's Humboldt current (e.g., Houston, 2006). Additionally, the Coastal Cordillera between the Central Depression and the Pacific Ocean minimizes the amount of moisture that can reach the Atacama. A north–south gradient in mean annual precipitation sets the boundaries of ecosystems. The hyperarid north (19–23°S) is largely abiotic, and increasing fog and precipitation from 26° to 29°S enables vegetation to begin taking hold near the southern extent of the desert (Navarro-Gonzalez et al., 2003; Rundel et al., 1991; Owen et al., 2011).

Our study is focused within the hyperarid central Atacama Desert, between 21°and 24°S (Fig. 1), an area that now experiences minimal winter rainfall ($<3 \, mm \, yr^{-1}$) sourced from the Pacific Ocean. Specifically, we centered our study around the 24°S latitude, near a boundary between moisture effects from two wind belts, the southern westerlies and the tropical easterlies (Maldonado et al., 2005). North of 24°S, most of the moisture carried by the tropical easterlies is excluded from the northern Atacama Desert by the rain

shadow of the Andes. During the summer, however, convective precipitation related to the South American Summer Monsoon can deliver moisture to the eastern edge of the northern Atacama Desert (Zhou and Lau, 1998; Ammann et al., 2001; Placzek et al., 2010). South of 24°S, precipitation thus increases with latitude and is delivered primarily in the form of winter precipitation from Pacific fronts and cutoff lows (Vuille and Ammann, 1997; Latorre et al., 2006; Placzek et al., 2010). The rare precipitation events that have delivered the minimal rainfall recorded near 24°S are most likely attributed to the interception of these cold air masses by increasingly high topography to the east of the Central Depression (Vuille and Ammann, 1997; Placzek et al., 2010). Any past shift in the boundary between these two moisture regimes would be significant to processes active across our study sites since they are near the modern boundary. Independent studies of the late Quaternary paleoclimate of northern Chile suggest that the northernmost boundary of Pacific-derived moisture has shifted toward the equator during recent glacial periods (Lamy et al., 1998; Lamy et al., 2000; Stuut and Lamy, 2004; Maldonado et al., 2005; Heusser et al., 2006). It is therefore possible that the magnitude of precipitation fluctuated to levels higher than that present for hyperarid sites located from 22°S to 24°S, including our study area.

The pace of hillslope and fluvial processes in the Atacama Desert is widely thought to be slower than most places on Earth. However, a growing regional catalog of erosion rates and exposure ages derived from TCN concentrations in bedrock, boulders, and sediment reveals active processes, likely of varying magnitude and duration, from the Miocene to the present (Dunai et al., 2005; Nishiizumi et al., 2005; Kober et al., 2009; Evenstar et al., 2009; Owen et al., 2011; Placzek et al., 2010; Amundson et al., 2012). Such studies also reveal that results from opposite ends of the cosmogenic nuclide-derived surface process rate spectrum mirror the modern day gradient of an increasingly hyperarid climate from 24°S northward. Dunai et al. (2005) reported a wide range of
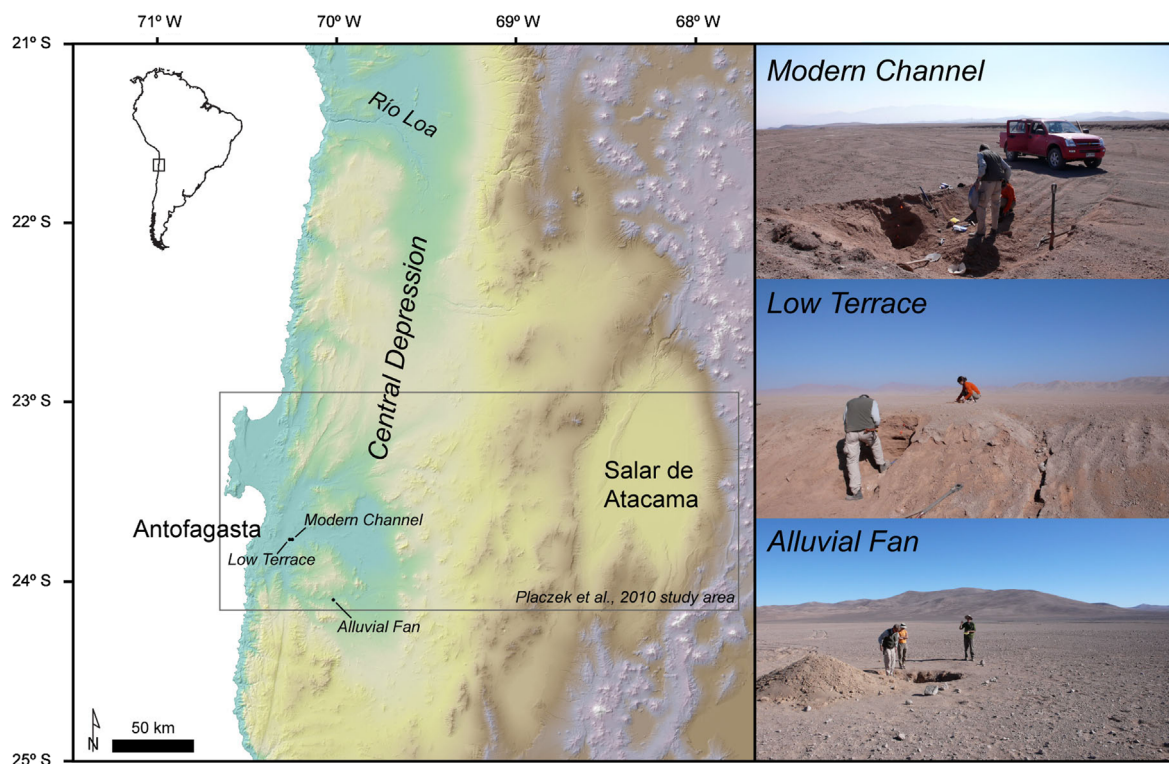


**Fig. 1.** Sample sites in the hyperarid Atacama Desert of northern Chile. Modern channel and low terrace profiles are east of Antofagasta in the Central Depression. The alluvial fan profile is farther south but within the same geological framework. Inset photographs show field setting for each sample site: modern channel ('Floating Man'), low terrace ('Dancing Bag'), and alluvial fan ('Yungay'). Please see Supplementary Fig. S1 and the Supplementary KMZ file to view higher resolution imagery of each site.

exposure ages, from 4 to 37 million yr, for surficial cobbles on an alluvial fan remnant in the northern Atacama Desert. The preservation of such relict landforms requires negligible erosion from their deposition to the present. Such low erosion rates are consistent with the extremely low probability of precipitation within the northern Atacama Desert, as predicted by the modern climate gradient. In contrast, Placzek et al. (2010) collected samples along a transect from the Andes, across the Central Depression, to the Coastal Cordillera, roughly parallel to ~24°S and reported minimum exposure age–maximum erosion rate pairs derived from $^{10}$Be, $^{26}$Al, and $^{21}$Ne concentrations that suggested active surface processes throughout the Pleistocene. Placzek et al. (2010) interpret low cosmogenic nuclide concentrations in fluvial sediment to mean that (1) sediment is not simply being derived from nearby, long-exposed boulders, and (2) surface processes must be active in the Pleistocene. Cyclical shifts of wetter conditions during the Quaternary may have driven the surface processes inferred by Placzek et al. (2010).

## 1.2. Study approach

Our goal is to quantify rates of Pliocene and Quaternary surface processes in the Atacama Desert. To do so, we sampled a TCN depth profile from a regionally extensive Plio-Pleistocene fill that was the focus of previous cosmogenic nuclide surface exposure studies (Ewing et al., 2006) and other isotopic studies investigating pedogenic processes (Ewing et al., 2007, 2008). We chose two additional sites to explore the nature of inset Quaternary features: (1) the modern channel of an active wash system; and (2) an adjacent terrace of the same system. These three field sites represent a chronosequence of the regional fluvial systems that span what is hypothesized to be a major climate and hydrological change in the late Pliocene (Wara et al., 2005).

Questions addressed by our data include: (1) how active are modern alluvial channels in the present hyperarid climate, (2) when did the fluvial network last incise into its alluvial bed, abandoning its lowest terraces, and (3) are the broad alluvial fans widely observed throughout the Central Depression still active, or are they stable, relict landforms related to a past climate?

## 2. Methods

### 2.1. Determining sediment deposition rates with TCN depth profiles

The rate and duration of sediment deposition, bioturbation, and erosion control the concentrations of cosmogenic nuclides as a function of depth within the upper few meters of an alluvial deposit (e.g., Lal and Arnold, 1985; Phillips et al., 1998; Granger and Riebe, 2007). Most commonly, TCN concentration depth profiles are used to infer the duration that a deposition surface has been stable. The determination of a surface exposure age for a fluvial terrace must account for 'inherited' TCN concentrations in sediment produced during exposure upstream from the terrace (Anderson et al., 1996):

$$N(z,t) = N_0 e^{-\lambda t} + \frac{P_0 e^{(-\rho z)/\Lambda}}{\lambda + (\rho \varepsilon/\Lambda)} (1 - e^{-(\lambda + (\rho \varepsilon/\Lambda))t}) \tag{1}$$

where $N$ is the cosmogenic nuclide concentration [atoms g$^{-1}$], $t$ is the time [yr], $N_0$ is the inherited concentration of the cosmogenic nuclide [atoms g$^{-1}$], $\varepsilon$ is the erosion rate [cm yr$^{-1}$] (assumed to be zero for our purposes), $\lambda$ is the decay constant for a radionuclide [yr$^{-1}$], $z$ is the depth below the deposit surface [cm], $P_0$ is the cosmogenic nuclide production rate at the surface [atoms g$^{-1}$ yr$^{-1}$], $\Lambda$ is the attenuation length for cosmogenic nuclide production [g cm$^{-2}$], and $\rho$ is the sediment density [g cm$^{-3}$].

In a few cases, profiles of TCNs with depth have not shown the expected relationship of an exponential decline with depth that is diagnostic of an attenuation profile produced during a period of stability. Rather, these profiles reflect an increase in TCN concentrations with depth (Clapp et al., 2001; Nichols et al., 2002). In such a case, the TCN concentration depth profiles can be used to infer steady-state deposition rates for the sediment by fitting the data to analytical models that quantify the TCN concentration as a function of depth and sediment deposition rate. The difference in form between a TCN concentration depth profile that is a function of deposition rate (Eq. (2)) vs. a function of exposure time and erosion rate (Eq. (1)) is clearly observable (Fig. 2).

Lal and Arnold (1985) first defined the steady-state solution for TCN concentrations in accumulating sediment as a function of depth and sedimentation rate:

$$N(z,D) = N_i e^{-\lambda z/D} + \frac{P_0}{(D\rho/\Lambda) - \lambda} (e^{-\lambda z/D} - e^{-\rho z/\Lambda}) \tag{2}$$

where $D$ is the deposition rate [cm yr$^{-1}$], $N_i$ is the cosmogenic nuclide concentration of sediment being deposited at the surface [atoms g$^{-1}$], and all other variables are as defined for Eq. (1). Note that this formulation of Lal and Arnold's solution accounts for decay of radionuclides unlike several later formulations (e.g., Phillips et al., 1998; Clapp et al., 2001; Nichols et al., 2002). Versions of Eq. (2) that do not account for decay are best suited for settings where erosion–deposition cycles are much shorter than the half-life of any cosmogenic radionuclide of interest. If sediment deposition rates are on the order of 1 m Myr$^{-1}$ or slower, as in the Atacama Desert, then radionuclide decay must be accounted for (Lal and Arnold, 1985).

Clapp et al. (2001) and Nichols et al. (2002) both reported sediment deposition rates from alluvial deposits in semi-arid landscapes of the American Southwest. Clapp et al. (2001) fitted their data to a deposition rate of 280 m Myr$^{-1}$ which implies that the 350 cm deep exposure of sediment that they sampled was deposited over approximately 12,500 yr. This inferred period of
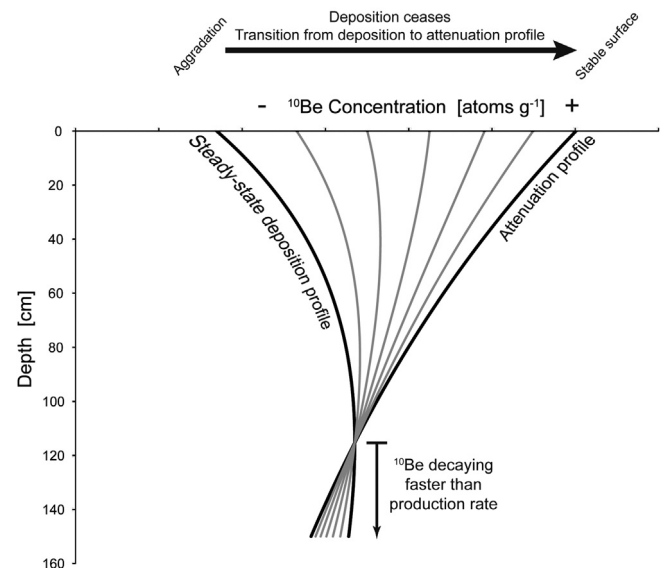


**Fig. 2.** Transition from a $^{10}$Be depth profile that is a function of deposition rate to a profile that is a function of exposure time and erosion rate. If sediment is steadily accumulating at a site, then $^{10}$Be concentrations increase with depth according to a characteristic depositional profile defined by Eq. (2). If an aggrading stream incises into its alluvial bed, the previously aggrading sediment becomes stable, and $^{10}$Be concentrations will begin to transition toward the more familiar attenuation profile, defined by Eq. (1), associated with surface exposure dating of alluvial deposits (e.g., Anderson et al., 1996).

deposition is much shorter than the half-life of $^{10}$Be (their nuclide of interest), so decay of $^{10}$Be was not an issue. Nichols et al. (2002) reported slightly slower deposition rates of 17 and 38 m Myr$^{-1}$, but these rates still suggested an erosion–deposition cycle shorter than the half-lives of their two target nuclides, $^{26}$Al and $^{10}$Be.

## 2.2. Sample collection and processing

At each site, we collected sediment at regular intervals from the land surface to depths of 75–200 cm. The maximum sampled depth was set by either sedimentary deposit boundaries, or by practical constraints on digging. Samples were first sieved to extract the 250–1000 μm fraction, and pebbles larger than 1000 μm were then crushed and sieved to bulk up the total amount of sample in the 250–1000 μm range since samples were not quartz-rich. We then isolated quartz via cleaning in aqua regia and subsequent etching in HF and HNO$_3$. We extracted $^{10}$Be through column chromatography, and $^{10}$Be/$^9$Be ratios were measured via accelerator mass spectrometry at the Purdue Rare Isotope Measurement Laboratory at Purdue University. Table 1 shows complete results.

We measured cosmogenic $^{21}$Ne at the Berkeley Geochronology Center by encapsulating 150 mg aliquots (of the same purified quartz analyzed for $^{10}$Be) in a Ta packet, heating them under vacuum using a 150 W diode laser, purifying the released gas by reaction with hot and/or cold getters and cryoseparation of Ne from other noble gases, and analyzing the resulting Ne in a MAP-215-50 mass spectrometer. Balco and Shuster (2009) describe analytical details. Table S1 shows complete results. Ne isotope ratios in all steps were indistinguishable from a two-component mixture of atmospheric and cosmogenic neon, so we computed cosmogenic Ne concentrations on this basis. Analyses of the CRONUS-A quartz standard during the period of these measurements yielded a cosmogenic $^{21}$Ne concentration of $338.9 \pm 3.8 \times 10^6$ atoms g$^{-1}$.

## 2.3. Modeling approach

We fit Eq. (2) to our observed TCN concentrations by determining the values of the free parameters $N_i$ and $D$ that minimized the chi-squared misfit between modeled values and our data:

$$M = \sum_{j=1}^{n} \left[ \frac{N(z_j, D) - N_j}{\sigma_j} \right]^2 \tag{3}$$

where $N(z_j, D)$ is the modeled cosmogenic nuclide concentration at depth $z_j$ and a given deposition rate, $N_j$ is the measured cosmogenic nuclide concentration at depth $z_j$, $\sigma_j$ is the one standard error analytical uncertainty at depth $z_j$, and $n$ is the number of samples in our profile. We utilize the 'fmincon' function of the MATLAB Optimization Toolbox to identify a minimum in an objective function

for fitting modeled deposition profiles to our data (see Supplementary material for example M-files).

## 3. Results and discussion

### 3.1. Late Pliocene fan ('Yungay')

To place the data from our younger field sites in a regional context, we first report the TCN profile from an alluvial fan that is part of a prominent regional depositional blanket into which Quaternary features are incised and deposited (Fig. 1). The Yungay site is on the distal end of alluvial fans derived from adjacent uplands and small mountains. Amundson et al. (2012) noted that these fans fill in, and thus postdate, early Pliocene or Miocene stream channels. In addition, the source areas of the fans (the surrounding uplands) are now encased in salt and dust, and are largely inactive as a sediment source. Based on these relations, Amundson et al. (2012) interpret the fan aprons around the uplands to be the result of regional response to the onset of hyperarid conditions, and the fans are composed of the sediment stripped from surrounding uplands as vegetation declined or disappeared during this regional aridification. Evidence supporting this hypothesis is that the surrounding uplands have little saprolite, and largely consist of salt fractured fresh igneous rock covered with sulfate/chloride/nitrate salts and silicate dust.

The age of the alluvial aprons are constrained at ~2.1–2.2 Myr by K–Ar or Ar–Ar dating of ash embedded within the upper meter of sediment in a deposit near our site (Ewing et al., 2006), and by $^{10}$Be concentrations of surface boulders/clasts (Ewing et al., 2006; Amundson et al., 2012). At the ash site, $^{10}$Be concentrations ranged from $6.27 \times 10^6$ to $1.13 \times 10^7$ atoms g$^{-1}$, yielding minimum apparent exposure ages from 0.988 to 2.42 Myr—ages consistent with the nearby ash dates. The range of apparent boulder ages is most likely a function of differences in boulders' exposure histories both prior to and after deposition. Such scatter in exposure ages combined with observations that the salt-laden soils have undergone at least partial surficial alteration by past climatic oscillations (Ewing et al., 2006) motivates the use of a TCN concentration depth profile through the soils and sediments to better constrain the age of the apron.

The depth profile of $^{10}$Be at Yungay decreases exponentially with depth from 0.5 m to 2 m, with the surface having the lowest $^{10}$Be concentration (Fig. 3). This pattern is suggestive of an attenuation profile that is truncated near the surface by an `active transport layer' as described by Nichols et al. (2002) for biotically and hydrologically active sites in the southwest United States. There is no evidence for biotic processes impacting the Yungay soil throughout its history, nor is there evidence of re-activation of

**Table 1**
Sample locations and cosmogenic nuclide concentrations.

| Sample ID | Latitude | Longitude | Elevation (m) | Depth (cm) | [$^{10}$Be] (atoms/g$_{qtz}$) | ± | [$^{21}$Ne] (atoms/g$_{qtz}$) | ± |
|---|---|---|---|---|---|---|---|---|
| CH-DB-000cm | −23.76426 | −70.26296 | 566 | 0 | 4.38E+06 | 1.28E+05 | 4.94E+07 | 1.49E+06 |
| CH-DB-050cm | −23.76426 | −70.26296 | 566 | 50 | 4.21E+06 | 1.88E+05 | 6.97E+07 | 3.31E+06 |
| CH-DB-100cm | −23.76426 | −70.26296 | 566 | 100 | 4.20E+06 | 6.02E+04 | 6.50E+07 | 3.03E+06 |
| CH-DB-150cm | −23.76426 | −70.26296 | 566 | 150 | 4.27E+06 | 2.01E+05 | 5.57E+07 | 2.05E+06 |
| CH-FM-000cm | −23.76484 | −70.24759 | 614 | 0 | 3.73E+06 | 8.12E+04 | 5.72E+07 | 3.84E+06 |
| CH-FM-025cm | −23.76484 | −70.24759 | 614 | 25 | 3.96E+06 | 1.15E+05 | 6.24E+07 | 3.06E+06 |
| CH-FM-050cm | −23.76484 | −70.24759 | 614 | 50 | 4.27E+06 | 1.29E+05 | 6.41E+07 | 3.21E+06 |
| CH-FM-075cm | −23.76484 | −70.24759 | 614 | 75 | 4.66E+06 | 2.04E+05 | 5.30E+07 | 2.25E+06 |
| CH-YG-000cm | −24.10161 | −70.01829 | 1009 | 0 | 6.98E+06 | 2.41E+05 | 8.33E+07 | 4.21E+06 |
| CH-YG-050cm | −24.10161 | −70.01829 | 1009 | 50 | 8.31E+06 | 1.66E+05 | 8.97E+07 | 3.99E+06 |
| CH-YG-100cm | −24.10161 | −70.01829 | 1009 | 100 | 7.92E+06 | 1.58E+05 | 9.66E+07 | 4.09E+06 |
| CH-YG-200cm | −24.10161 | −70.01829 | 1009 | 200 | 7.54E+06 | 1.61E+05 | n/a | n/a |
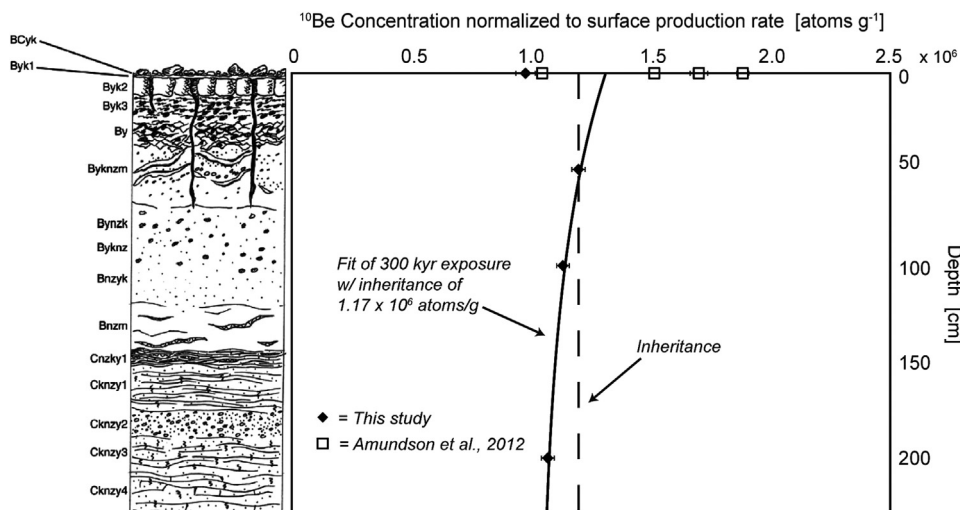
**Fig. 3.** [10]Be depth profile for Yungay soil (error bars are 1σ analytical error) with soil profile sketch and description (Ewing et al., 2006) for context. [10]Be concentrations jump to higher concentrations at 50 cm below the surface, and then decay with depth. Surface concentrations are similar to those reported by Ewing et al. (2006). A best-fit exposure age for this profile using Eq. (1) suggests an apparent exposure age of 300,000 yr.
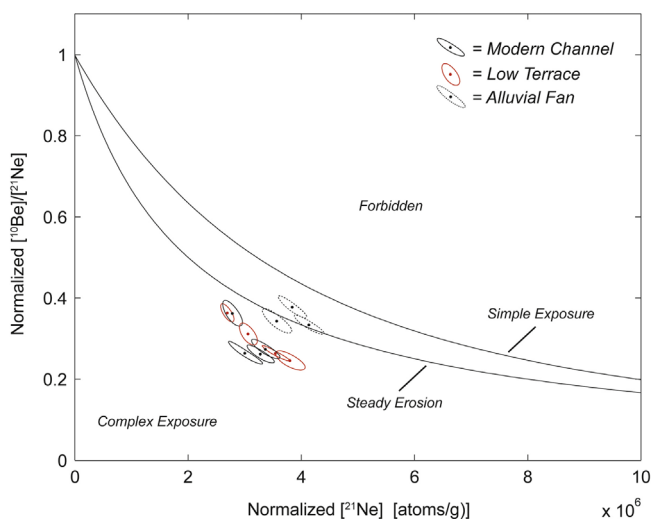


**Fig. 4.** Lal 'erosion island' plot for [10]Be/[21]Ne ratios of modern channel, low terrace, and alluvial fan samples. Concentrations above the simple exposure (i.e., no erosion) line are not possible. Steady erosion line is a continuum of steady-state erosion endpoints. Concentrations between the simple exposure curve and the steady erosion curve are within the 'island' of simple exposure and erosion. Concentrations below the steady erosion continuum are the result of repeated burial and re-exposure or constant burial. Samples from the modern channel and low terrace profiles have undergone a complex exposure history during transport within the Central Depression. Samples from the alluvial fan profile appear to have undergone only one cycle of erosion and deposition. Sixty-eight percent confidence ellipses for analytical error.

distributary channels. However, the upper few tens of centimeters appear to be composed of more recent dust and sulfate salt overlain upon a dense sulfate horizon that may have been truncated, or at least modified, by more pluvial intervals (Quade et al., 2008). At Yungay, these intervals must not have been so humid or prolonged as to remove the salts in the profile.

We model the evolution of [10]Be and [21]Ne concentrations in sediment undergoing either simple exposure or steady erosion (Fig. 4). If sediment is buried and shielded from further TCN production, the continued radioactive decay of [10]Be moves the sediment's TCN signature from the steady state erosion island (Lal, 1991) into the 'complex exposure' field. [10]Be/[21]Ne ratios for sediment in the Yungay profile plot within the steady state erosion island, suggesting rapid erosion of the sediment from the uplands and deposition in the Yungay fan complex. This is consistent with

the hypothesis of Amundson et al. (2012) of a relatively rapid geomorphic response to a profound climate change near 2.2–2.0 Myr, one that is contemporaneous with the onset of the Pacific ENSO cycle (Wara et al., 2005).

It is important to note that, considered without the underlying profile, our surface sample's [10]Be concentration of $6.98 \pm 0.241 \times 10^6$ atoms g$^{-1}$ would suggest a minimum exposure age of ~1.4 Myr. This age agrees with previously reported exposure ages of 0.92–2.1 Myr inferred from surface samples at the same site (Amundson et al., 2012). Fitting the truncated attenuation profile with Eq. (1) (using exposure time and inheritance as free parameters and assuming no erosion) suggests, however, an apparent exposure age of approximately 300,000 yr and an inheritance of $8.4 \times 10^6$ atoms g$^{-1}$ (Fig. 3). We take this 300,000 yr as an extreme minimum for the timing of this fan surface's abandonment, with a maximum age of ~2 Myr for the deposit inferred from the ash dated in a loosely correlative fan deposit 16 km to the southwest (Ewing et al., 2006). This difference between the fan's maximum and minimum age estimates is expected. Surface exposure dates derived from TCN concentrations in alluvial deposits provide minimum estimates for a surface's age by definition (Gosse and Phillips, 2001), and even slow erosion of the surface will have a large effect on a deposit's apparent exposure age. A study investigating young displacement on the Atacama Fault System reported a similar result in dating alluvial fans 15–20 km to the northwest of our site (Gonzalez et al., 2006). Gonzalez et al. (2006) measured [21]Ne quartz clasts from the surfaces of abandoned alluvial fans, and they correct for [21]Ne inheritance by subtracting TCN abundances measured in modern channel sand collected from each fan's source catchment from surface clasts' [21]Ne concentration. Apparent exposure ages derived from corrected [21]Ne concentrations ranged from 350,000 to 550,000 yr, in contrast to maximum ages of 3–5 Myr for the bajada derived from ashes 1–3 m below the fan's surfaces. Our data and that of Gonzalez et al. suggest that an effort should be made to constrain deposits' TCN inheritance when determining surface exposure ages in the Atacama Desert.

### 3.2. Modern channel ('Floating Man')

We selected a wash system incised into the regional alluvial deposits (Fig. 1) to determine both the long term stability of these systems and to better understand their sediment sourcing and
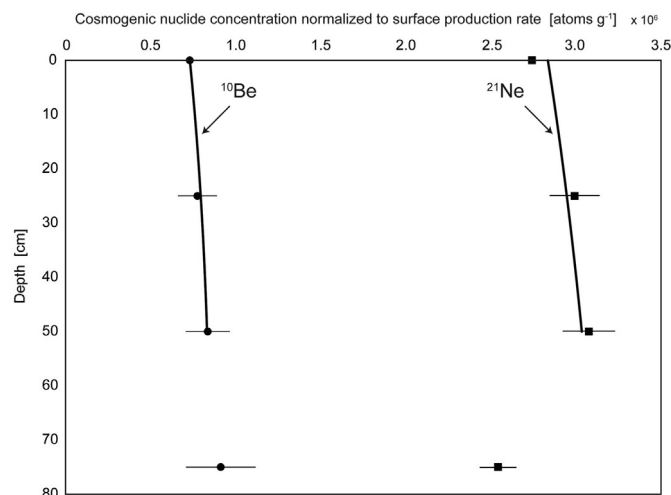
**Fig. 5.** $^{10}$Be and $^{21}$Ne depth profiles for modern channel site ('Floating Man'). Cosmogenic nuclide concentrations increase as a function of depth suggesting a depositional profile (error bars are $1\sigma$ analytical error and smaller than the symbols for the $^{10}$Be data). We infer a best-fit deposition rate of $2.1 \pm 1.0$ m Myr$^{-1}$ for both nuclide profiles. This rate requires a minimum period of aggradation of 250,000 yr for this site (i.e., 0.5 m Myr/2.1 m). Error bars are $1\sigma$ analytical uncertainty.

cycling. We begin by examining the active wash (named 'Floating Man' in the field).

In the modern channel, $^{10}$Be and $^{21}$Ne concentrations increase as a function of depth into the channel's alluvial bed (Fig. 5). This pattern is the reverse of an attenuation profile that develops in a stable soil (see Yungay above), and is consistent with TCN concentrations that develop in alluvium aggrading at a relatively constant rate. Surface concentrations are lowest and should be a function of either the upland erosion rates (Brown et al., 1995; Bierman and Steig, 1996; Granger et al., 1996) or the exposure history of the sediment being sourced by the fluvial system. Progressively deeper samples accumulate TCNs at lower and lower production rates until they are completely shielded by burial from further nuclide production. We fit the $^{10}$Be and $^{21}$Ne profiles to solutions for Eq. (2) to identify the best-fit values for $^{10}$Be and $^{21}$Ne at the surface and a best-fit deposition rate. The data are best described by inherited $^{10}$Be and $^{21}$Ne concentrations of $3.72 \pm 0.076 \times 10^6$ atoms g$^{-1}$ and $59.3 \pm 1.90 \times 10^6$ atoms g$^{-1}$, respectively, and a deposition rate of $2.1 \pm 1.0$ m Myr$^{-1}$. We fit only the upper three samples for each nuclide at this site because the $^{10}$Be/$^{21}$Ne ratio for the deepest sample is significantly different from the overlying samples' $^{10}$Be/$^{21}$Ne ratios (Fig. 4), suggesting a different sediment source. A variation in sediment source, and associated cosmogenic nuclide concentrations, would violate the assumption of a consistent input concentration at the profile's surface which Eq. (2) requires. Our model suggests that the upper 50 cm of sediment accumulated over approximately 250,000 yr. Since it is possible that this deposition profile continues below our deepest sample, 250,000 yr is a minimum estimate for the duration of the current aggradation within the wash. We note that including the $^{10}$Be concentrations at 75 cm does not significantly affect the best-fit deposition rate for this site. If the deepest sample is included in the deposition model, then this profile reflects 375,000 yr of deposition.

The $^{10}$Be/$^{21}$Ne ratios for samples in the modern channel require intermittent burial and shielding of the sediment during its transport through the fluvial system (Fig. 4). This complex exposure history for sediment in the modern channel is indicative of two important features for this Quaternary fluvial system: (1) sediment is being sourced from older alluvial deposits that have undergone at least one episode of exposure and burial. This scenario is consistent with our observations that hillslopes provide little sediment and the modern washes largely tap and rework older alluvial fan deposits. (2) The cut–fill nature of this system reflects cycles of sediment transport (exposure), deposition (shielding), and remobilization (re-exposure) in the drainage network during the Quaternary.

### 3.3. Stream terrace ('Dancing Bag')

Adjacent to the active wash is a small terrace remnant inset into the regional, Pliocene alluvium (Fig. 1). We examined an exposure of this terrace created by the present wash. The profile revealed ~50 cm of relatively unweathered alluvium over a salt-cemented hardpan. The field interpretation of this stratigraphy is that the incising stream truncated the well-developed soil (Ewing et al., 2006) in the alluvial fan down to a restrictive layer and left an overlying cap of more recent sediment. The adjacent wash was at some point able to breach the salt-cemented layer, incise, and is now aggrading (as discussed in the previous section).

Unlike the other two sites, the $^{10}$Be concentrations in the terrace are constant as a function of depth. A constant relationship between cosmogenic nuclide and depth is not uncommon in a well-mixed upland soil (Jungers et al., 2009), but it is unusual and unexpected in a physically stable surface such as an abandoned fluvial fill terrace in an abiotic environment. Previous work suggests two possible scenarios for the development of a depth-invariant cosmogenic nuclide profile:

(1) Mixing of sediment by biota (gophers, ants, worms, trees, etc.) produces a constant relationship between cosmogenic nuclide concentrations and depth (Perg et al., 2001; Granger and Riebe, 2007; Jungers et al., 2009) because the timescale of mixing is significantly shorter than the time needed to develop the cosmogenic nuclide attenuation profile of Fig. 2.
(2) Cosmogenic nuclide concentrations in well-mixed fluvial sediment deposited very recently and rapidly will be depth-invariant since the sediment would represent an averaged sample of sediment from the eroding uplands (Anderson et al., 1996). Such a deposit must be younger than approximately 100,000 yr (at this site's latitude and elevation) to have not developed a cosmogenic nuclide attenuation profile.

The setting of our stream terrace site seems to preclude both of these possibilities. First, there is no biota, a requirement of scenario 1. Second, the roughly constant cosmogenic nuclide concentration profile with depth at this terrace is similar to the concentrations observed in the modern channel, which could only be possible under scenario 2 if the terrace was deposited effectively 'yesterday'.

We approach the interpretation of this somewhat unusual TCN depth profile by leveraging our knowledge of when the modern channel incised below the terrace's surface. We have determined that the cosmogenic nuclide profile in the modern channel is best explained by a steady-state deposition rate of 2.1 m Myr$^{-1}$, and this requires that the channel incised below this terrace site and has subsequently been aggrading for at least 250,000 yr. Using this known minimum estimate for the duration of stability for the sampled terrace, we solve Eq. (1) for $N_0$, which provides an initial condition for each of our sampled depths. Note that $N(z,t)$ is the observed concentration for each depth in our profile. We find that the initial condition for this terrace's sediment was a steady-state deposition profile similar in form to the profile observed in the modern, aggrading channel (Fig. 6). The best-fit deposition rate for the terrace's initial condition is approximately 2 m Myr$^{-1}$, a rate in agreement with the modern rate of 2.1 m Myr$^{-1}$. Thus, we infer that (1) deposition rate for this fluvial system during its previous aggradation cycle was nearly the same as the modern rate, (2) the 150 cm thick package of sediment preserved in this terrace was
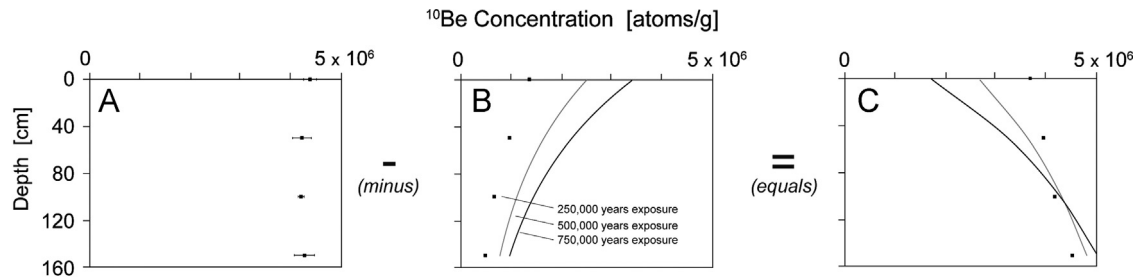
**Fig. 6.** The initial condition (pre-abandonment) for sediment at our low terrace site is determined by leveraging our knowledge of how long the adjacent channel has been aggrading subsequent to its incision below the terrace level. Solving Eq. (1) for $N_0$ finds the pre-incision [10]Be concentrations for each sample depth (C). This initial condition is essentially the result of subtracting the amount of [10]Be produced during terrace stability (B) from the observed [10]Be profile (A). Since 250,000 yr of exposure is a minimum estimate derived from the modern channel cosmogenic nuclide depth profile, we also include two longer exposure scenarios. However, initial conditions inferred from the 500,000 and 750,000 yr exposure scenarios suggest deposition profiles that are not reasonably explained by Eq. (2)—i.e., they would require deposition rates one to two orders of magnitude slower than even the very slow rates we observe at our modern channel site. The best fit deposition rate for the initial condition inferred from the 250,000 yr exposure scenario is 2 m Myr$^{-1}$.
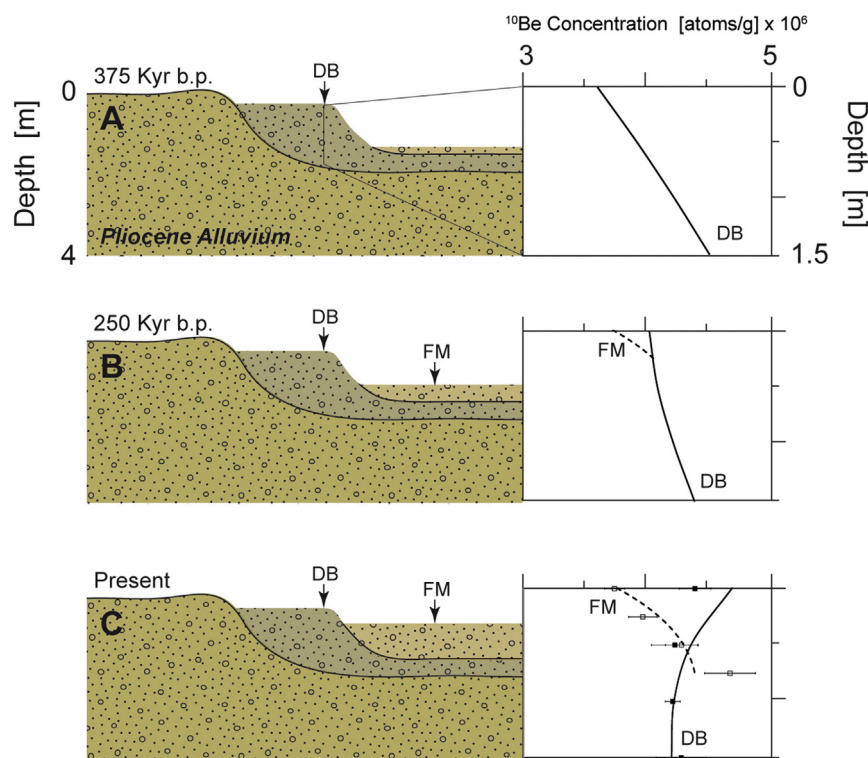


**Fig. 7.** Process model for the relationship between the modern channel site ('Floating Man' or FM) and the adjacent low terrace ('Dancing Bag' or DB). Note that for this model we include the deepest sample from the FM profile, so aggradation in the modern channel begins at 375,000 yr before present. Prior to 375,000 yr, the fluvial system had incised into Tertiary fill deposits, and subsequently aggraded for as long as 750,000 yr to produce the initial condition for the DB [10]Be profile (A). At 375,000 yr, the fluvial system incised below the DB terrace, and aggradation began. By 250,000 yr b.p. (B), 25 cm of sediment has aggraded in the modern channel and a steady-state deposition profile is developing for [10]Be in the FM sediment (dashed line). [10]Be concentrations in the terrace sediment (solid line) are transitioning from a deposition profile to an attenuation profile following 125,000 yr of stability. At present (C), 75 cm of sediment has accumulated in the modern channel, and continued deposition maintains a deposition profile for the [10]Be in the FM sediment (open boxes are observed concentrations, dashed line is modeled concentrations). [10]Be concentrations in the low terrace sediment (DB) continue transitioning toward an attenuation profile diagnostic of surface stability (closed boxes are observed concentrations, solid line is modeled concentrations). Error bars represent $1\sigma$ analytical uncertainty.

deposited over a period of 750,000 yr, and (3) during the past ~250,000 yr of stability, the cosmogenic nuclide concentration depth profile has transitioned from a steady-state deposition profile toward an attenuation profile, leading to a roughly depth-invariant isotopic profile. It is also possible that the terrace deposit is composed of more than one depositional unit. If deposition in the terrace was limited to the sediment above the stratigraphic discontinuity at 50 cm (the salt-cemented layer), then the inferred duration of deposition for terrace sediment is only 250,000 yr prior to terrace abandonment. A process model summarizes the relationship between deposition and erosion cycles and [10]Be concentrations for both the low terrace and modern channel sites (Fig. 7).

Further information about this profile and its sediment can be interpreted from the [10]Be/[21]Ne ratios. The [10]Be/[21]Ne ratios, like that of the channel, suggest complex exposure histories that would be expected from repeated reworking of sediment as it moves through this alluvial system from source to sink (Fig. 4).

## 4. Conclusions

We use [10]Be and [21]Ne concentration depth profiles in a chrono-sequence of alluvial features in the Atacama Desert to quantify changes in the rates of surface processes and the sources of

sediment from the late Pliocene to the present. A TCN profile from a ~2 Myr alluvial fan is consistent with the rapid erosion and deposition of sediment from upland rock and saprolite exposed in the local watershed in response to the onset of hyperaridity at the Plio-Pleistocene boundary. Occasional moisture and eolian processes reworked the upper centimeters of the fan since the Pliocene.

In contrast to the Plio-Pleistocene fans, Quaternary washes and terraces have sediment with complex exposure histories, suggestive of a reworking of soils from the ancient alluvial fans rather than a tapping of upland bedrock. A TCN profile in a modern channel reveals active fluvial aggradation of 2.1 m Myr$^{-1}$. On a small fluvial terrace above the modern channel that is partially incised into the adjacent ancient fans, we interpret the $^{10}$Be profile to represent ~250,000–375,000 yr of exposure history. Prior to terrace abandonment, the fluvial system aggraded 2 m Myr$^{-1}$ for ~250,000–750,000 yr before abandonment.

In summary, while fluvial activity has continued in this region of the Atacama Desert throughout the Quaternary, the nature of these processes and their rates appear to have undergone a fundamental change at approximately the Plio-Pleistocene boundary. Pre-Quaternary erosion and sedimentation linked upland bedrock and hillslopes to fluvial systems, potentially culminating in a stripping of hillslope sediment and the deposition of widespread fan complexes near the end of the Pliocene. The large alluvial deposits created in the Tertiary have largely been preserved and have experienced a nearly uninterrupted duration of soil formation via salt accumulation. In contrast, Quaternary processes have been remarkably slow and of a different nature. The Quaternary fluvial systems appear to source sediment from the ancient fans, and impact only a small fraction of the total watershed of which they are a part. The TCN concentrations within a typical Quaternary system indicate oscillations between incision and aggradation, and these processes are ongoing under the present, hyperarid climate. The most recent erosion–deposition cycle for our study area began between 250,000 and 400,00 yr ago, and we note that this is coincident with the especially cold stadials associated with MIS 10 and MIS 12 at 340,000 and 420,000 yr ago, respectively (Bard and Rickaby, 2009). If the subtropical front was pushed farther north than normal during these cooler periods, then it is possible that the associated increased moisture, and likely precipitation, at 24°S could have initiated the most recent incision event for this study's fluvial system.

## Acknowledgments

## Appendix A.  Supplementary materials

Supplementary data associated with this article can be found in the online version at http://dx.doi.org/10.1016/j.epsl.2013.04.005.

## References

Ammann, C., Jenny, B., Kammer, K., Messerli, B., 2001. Late Quaternary Glacier response to humidity changes in the arid Andes of Chile (18–29 degrees S). Palaeogeogr. Palaeoclimatol. Palaeoecol. 172, 313–326.

Amundson, R., Dietrich, W., Bellugi, D., Ewing, S., Nishiizumi, K., Chong, G., Owen, J., Finkel, R., Heimsath, A., Stewart, B., 2012. Geomorphologic evidence for the late Pliocene onset of hyperaridity in the Atacama Desert. Geol. Soc. Am. Bull. 124, 1048–1070.

Anderson, R.S., Repka, J.L., Dick, G.S., 1996. Explicit treatment of inheritance in dating depositional surfaces using in situ Be-10 and Al-26. Geology 24, 47–51.

Balco, G., Shuster, D.L., 2009. Production rate of cosmogenic Ne-21 in quartz estimated from Be-10, Al-26, and Ne-21 concentrations in slowly eroding Antarctic bedrock surfaces. Earth Planet. Sci. Lett. 281, 48–58.

Bard, E., Rickaby, R.E.M., 2009. Migration of the subtropical front as a modulator of glacial climate. Nature 460, U380–U393.

Bierman, P., Steig, E.J., 1996. Estimating rates of denudation using cosmogenic isotope abundances in sediment. Earth Surface Processes and Landforms 21, 125–139.

Brown, E.T., Stallard, R.F., Larsen, M.C., Raisbeck, G.M., Yiou, F., 1995. Denudation Rates Determined from the Accumulation of In Situ-Produced Be-10 in the Luquillo Experimental Forest, Puerto Rico. Earth and Planetary Science Letters 129, 193–202.

Carrizo, D., Gonzalez, G., Dunai, T., 2008. Neogene constriction in the northern Chilean Coastal Cordillera: neotectonics and surface dating using cosmogenic Ne-21. Rev. Geol. Chile 35, 1–38.

Clapp, E.M., Bierman, P.R., Nichols, K.K., Pavich, M., Caffee, M., 2001. Rates of sediment supply to arroyos from upland erosion determined using in situ produced cosmogenic Be-10 and Al-26. Quat. Res. 55, 235–245.

Dunai, T.J., Lopez, G.A.G., Juez-Larre, J., 2005. Oligocene–Miocene age of aridity in the Atacama Desert revealed by exposure dating of erosion-sensitive landforms. Geology 33, 321–324.

Evenstar, L.A., Hartley, A.J., Stuart, F.M., Mather, A.E., Rice, C.M., Chong, G., 2009. Multiphase development of the Atacama Planation Surface recorded by cosmogenic He-3 exposure ages: implications for uplift and Cenozoic climate change in western South America. Geology 37, 27–30.

Ewing, S.A., Sutter, B., Owen, J., Nishiizumi, K., Sharp, W., Cliff, S.S., Perry, K., Dietrich, W., McKay, C.P., Amundson, R., 2006. A threshold in soil formation at Earth's arid hyperarid transition. Geochimica Et Cosmochimica Acta 70, 5293–5322.

Ewing, S. A., G. Michalski, M. Thiemens, R. C. Quinn, J. L. Macalady, S. Kohl, S. D. Wankel, C.Kendall, C. P. McKay, and R. Amundson (2007), Rainfall limit of the N cycle on Earth, Global Biogeochem. Cycles 21, GB3009, http://dx.doi.org/10.1029/2006GB002838.

Ewing, S.A., Yang, W., DePaolo, D.J., Michalski, G., Kendall, C., Stewart, B.W., Thiemens, M., Amundson, R., 2008. Non-biological fractionation of stable Ca isotopes in soils of the Atacama Desert, Chile. Geochim. Cosmochim. Acta 72, 1096–1110.

González L., G., T. Dunai, D. Carrizo, and R. Allmendinger (2006), Young displacements on the Atacama Fault System, northern Chile from field observations and cosmogenic 21Ne concentrations, Tectonics 25, TC3006, http://dx.doi.org/10.1029/2005TC001846.

Gosse, J.C., Phillips, F.M., 2001. Terrestrial in situ cosmogenic nuclides: theory and application. Quaternary Science Reviews 20, 1475–1560.

Granger, D.E., Kirchner, J.W., Finkel, R., 1996. Spatially averaged long-term erosion rates measured from in situ-produced cosmogenic nuclides in alluvial sediment. Journal of Geology 104, 249–257.

Granger, D., Riebe, C., 2007. Cosmogenic Nuclides in Weathering and Erosion. Treatise on Geochemistry. Pergamon, Oxford, pp. 1–42.

Heusser, L, Heusser, C., Mix, A., McManus, J., 2006. Chilean and Southeast Pacific paleoclimate variations during the last glacial cycle: directly correlated pollen and delta 18O records from ODP Site 1234. Quat. Sci. Rev. 25, 3404–3415.

Houston, J., 2006. Variability of precipitation in the Atacama desert: its causes and hydrological impact. Int. J. Climatol. 26, 2181–2198.

Jungers, M.C., Bierman, P.R., Matmon, A., Nichols, K., Larsen, J., Finkel, R., 2009. Tracing hillslope sediment production and transport with in situ and meteoric Be-10. J. Geophys. Res.—Earth Surf., 114.

Kober, F., Ivy-Ochs, S., Zeilinger, G., Schlunegger, F., Kubik, P.W., Baur, H., Wieler, R., 2009. Complex multiple cosmogenic nuclide concentration and histories in the arid Rio Lluta catchment, northern Chile. Earth Surf. Process. Landforms 34, 398–412.

Lal, D., Arnold, J., 1985. Tracing quartz through the environment. J. Earth Syst. Sci. 94, 1–5.

Lamy, F., Hebbeln, D., Wefer, G., 1998. Late quaternary precessional cycles of terrigenous sediment input off the Norte Chico, Chile (27.5 degrees S) and palaeoclimatic implications. Palaeogeogr. Palaeoclimatol. Palaeoecol. 141, 233–251.

Lamy, F., Klump, J., Hebbeln, D., Wefer, G., 2000. Late Quaternary rapid climate change in northern Chile. Terra Nova 12, 8–13.

Latorre, C., Betancourt, J.L., Arroyo, M.T.K., 2006. Late Quaternary vegetation and climate history of a perennial river canyon in the Rio Salado basin (22 degrees S) of Northern Chile. Quat. Res. 65, 450–466.

Maldonado, A., Betancourt, J.L., Latorre, C., Villagran, C., 2005. Pollen analyses from a 50,000-yr rodent midden series in the southern Atacama Desert (25 degrees 30′S). J. Quat. Sci. 20, 493–507.

Navarro-Gonzalez, R., Rainey, F.A., Molina, P., Bagaley, D.R., Hollen, B.J., de la Rosa, J., Small, A.M., Quinn, R.C., Grunthaner, F.J., Caceres, L., Gomez-Silva, B., McKay, C.P., 2003. Mars-like soils in the Atacama Desert, Chile, and the dry limit of microbial life. Science 302, 1018–1021.

Nichols, K.K., Bierman, P.R., Hooke, R.L., Clapp, E.M., Caffee, M., 2002. Quantifying sediment transport on desert piedmonts using Be-10 and Al-26. Geomorphology 45, 105–125.

Nishiizumi, K., Caffee, M.W., Finkel, R.C., Brimhall, G., Mote, T., 2005. Remnants of a fossil alluvial fan landscape of Miocene age in the Atacama Desert of northern Chile using cosmogenic nuclide exposure age dating. Earth Planet. Sci. Lett. 237, 499–507.

Owen, J.J., Amundson, R., Dietrich, W.E., Nishiizumi, K., Sutter, B., Chong, G., 2011. The sensitivity of hillslope bedrock erosion to precipitation. Earth Surf. Processes Landforms 36, 117–135.

Perg, L.A., Anderson, R.S., Finkel, R.C., 2001. Use of a new Be-10 and Al-26 inventory method to date marine terraces, Santa Cruz, California, USA. Geology 29, 879–882.

Phillips, W.M., McDonald, E.V., Reneau, S.L., Poths, J., 1998. Dating soils and alluvium with cosmogenic Ne-21 depth profiles: case studies from the Pajarito Plateau, New Mexico, USA. Earth Planet. Sci. Lett. 160, 209–223.

Placzek, C.J., Matmon, A., Granger, D.E., Quade, J., Niedermann, S., 2010. Evidence for active landscape evolution in the hyperarid Atacama from multiple terrestrial cosmogenic nuclides. Earth Planet. Sci. Lett. 295, 12–20.

Quade, J., Rech, J.A., Betancourt, J.L., Latorre, C., Quade, B., Rylander, K.A., Fisher, T., 2008. Paleowetlands and regional climate change in the central Atacama Desert, northern Chile. Quat. Res. 69, 343–360.

Rundel, P.W., Dillon, M.O., Palma, B., Mooney, H.A., Gulmon, S.L., Ehleringer, J.R., 1991. The phytogeography and ecology of the Coastal Atacama and Peruvian Deserts. Aliso 13, 1–50.

Stuut, J.B.W., Lamy, F., 2004. Climate variability at the southern boundaries of the Namib (Southwestern Africa) and Atacama (northern Chile) coastal deserts during the last 120,000 yr. Quat. Res. 62, 301–309.

Vuille, M., Ammann, C., 1997. Regional snowfall patterns in the high, arid Andes. Climatic Change 36, 413–423.

Wara, M.W., Ravelo, A.C., Delaney, M.L., 2005. Permanent El Nino-like conditions during the Pliocene warm period. Science 309, 758–761.

Zhou, J.Y., Lau, K.M., 1998. Does a monsoon climate exist over South America? J. Clim. 11, 1020–1040.